

# Matched Decoding for Punctured Convolutional Encoded Transmission Over ISI-Channels

Fabian Schuh, Andreas Schenk, and Johannes B. Huber

Institute for Information Transmission, Friedrich-Alexander-Universität Erlangen-Nürnberg, Germany

mail: {schuh, schenk, huber}@LNT.de

**Abstract**—Matched decoding is a technique that enables the efficient maximum-likelihood sequence estimation of convolutionally encoded PAM-transmission over ISI-channels. Recently, we have shown that the super-trellis of encoder and channel can be described with significantly fewer states without loss in Euclidean distance, by introducing a non-linear representation of the trellis. This paper extends the matched decoding concept to punctured convolutional codes and introduces a time-variant, non-linear trellis description.

**Index Terms**—ISI-channel; punctured convolutionally encoded transmission; super-trellis decoding; matched decoding;

## I. INTRODUCTION

Coded pulse-amplitude modulation poses an attractive digital transmission scheme when low over-all delay is desired but the channel induces intersymbol interference (ISI). Low latency is obtained by the use of convolutional codes instead of block codes (*cf.* [1]) and dispense with interleaving (as opposed to convolutional bit-interleaved coded modulation [2]).

Punctured codes are widely used in applications where high code rates are required. With puncturing, a convolutional code with high code rate can be derived from *mother code* with a low code rate. At the receiver, equalization and decoding are usually performed subsequently in two separate processing steps, each based on its own trellis description. After equalization,<sup>1</sup> bit probability  $1/2$  are inserted before decoding when symbols are punctured.

In [3] we proposed a matched decoding scheme where super-trellis decoding of the ISI-channel and *non-punctured* convolutional encoding is performed jointly on a reduced number of states. There, the output of the rate- $K/n$  convolutional encoder was mapped onto  $M = 2^n$  symbols directly following the concept of trellis coded modulation. In our setup, we will perform equalization of the ISI-channel and decoding of the punctured convolutional code jointly in a single super-trellis [4]. This technique, however, is commonly not applied practically due to the large overall number of states of a super-trellis as well as the complex finite state machine to represent the encoding with a punctured convolutional code. However, we show how to extend the matched decoding (MD) concept to the use with punctured convolutional codes and therefore

This work was supported by Bundesministerium für Wirtschaft und Technologie (BMWi) within the project C-PMSE.

<sup>1</sup>The bit metrics of punctured symbols are set to an erasure (*e.g.*,  $\mathcal{L} = 0$ ) before decoding.

reduce the total number of states. For this, we will first show how to describe the encoding with a punctured code as a finite state machine (FSM), only, and extend it to compute the hypotheses for the punctured convolutional code transmitted over an ISI-channel. We will show that the trellis described by the extended FSM is time-variant and can be used for decoding using a modified version of the Viterbi algorithm (VA) [5].

The paper is organized as follows: After the definition of the system model for punctured convolutional coded transmission over ISI-channels in Sec. II, we will first describe the FSM for *non-punctured* convolutional codes and briefly recall matched decoding in Sec. III. In Sec. IV we will describe the FSM for punctured codes and extend our MD approach. Numerical simulations are shown in Sec. V. The paper concludes with a summary.

## II. SYSTEM MODEL

We first introduce the system model for a convolutionally encoded PAM transmission over ISI-channel (*cf.* discrete-time example of Fig. 1).

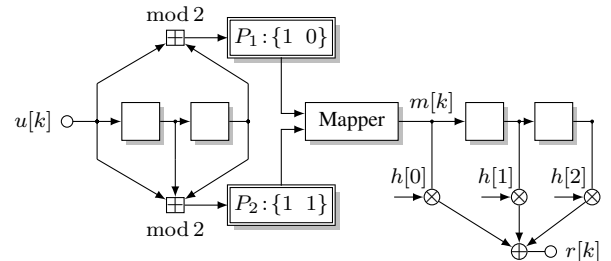


Fig. 1: System model for a encoded 4-ary transmission over ISI-channels with a punctured convolutional code and overall rate  $R = 4/3$ .

The transmitter is composed of a rate- $K/n$  binary convolutional encoder with generator polynomials  $[g_{ij}]$ ;  $1 \leq i \leq n$ ;  $1 \leq j \leq K$ , with  $K$  input symbols and  $n$  parallel output symbols at each time instant. At each output branch of the encoder, the symbols traverses through a non-linear time-invariant puncturing system with periodic puncturing scheme  $P_i$ ;  $1 < i \leq n$ . For each encoder input symbol the puncturing scheme cyclically advances by one step. Whenever the scheme is zero, the current symbol at the output gets punctured (*i.e.*, discarded), accordingly. The punctured output is mapped for a  $M$ -ary PAM transmission. The transmit signal traverses

through a memory- $L$  discrete-time ISI-channel with  $L + 1$  channel coefficients  $h[k]$  with  $k$  denoting the time index.

The only requirement necessary for the matched decoding approach is that the rate- $K/n$  convolutional code is matched to the  $M$ -ary modulation via  $M = 2^n$ . For sake of simplicity, we here consider real-valued ASK, only. For clarity, we restrict ourselves to  $M = 4$ , but note that the concept can be extended to arbitrary  $M = 2^n$ .

### III. MATCHED DECODING OF NON-PUNCTURED CODES

In order to introduce maximum-likelihood sequence estimation (MLSE) for punctured codes, we first describe the encoding and mapping process for *non-punctured* convolutional encoding and natural labeling. We first ignore the ISI-channel for simplicity, *i.e.*,  $L = 0$ , and later briefly recall our MD approach also considering an ISI-channel. Please note that here a single uncoded bit is encoded with a rate- $1/2$  convolutional encoder resulting in two coded bits, *i.e.*, MSB and LSB, respectively. These coded bits contain the information of a single uncoded bit and are mapped onto a single transmit symbol  $m[k]$ . Thus, after mapping, the overall rate of the transmission is  $R = 1^{\text{bit/symbol}}$ .

#### A. Description of the Finite State Machine

Fig. 2 illustrates the encoding process (top) and the state transitions of the FSM (bottom) when no puncturing is involved. The uncoded unipolar information sequence  $u[k] \in \{0, 1\}$  is inserted into the FSM (light gray,  $\square$ ) as input values and later passes through all delay elements describing the state of the FSM (dark gray,  $\blacksquare$ ). Here, the generator polynomials  $g_i$ ,  $1 < i < 2$ , process the input symbol together with the FSM state synchronously at each time instant. The resulting encoded bits, denoted with MSB and LSB, respectively, are naturally labeled and mapped to the 4-ary symbol alphabet of the transmission scheme, *e.g.*, via  $m = 2(2\text{MSB} + \text{LSB}) - 1$ .

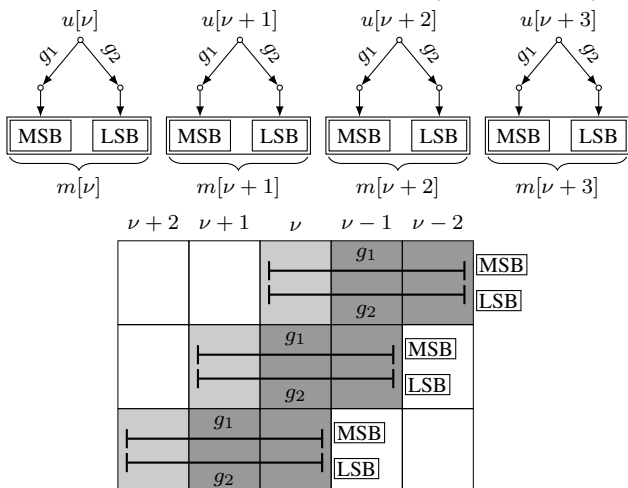


Fig. 2: Top: Encoding process for a rate- $1/2$  convolutional code and 4-ary mapping. Overall transmission rate  $R = 1$ . Bottom: State transitions of the transmitter FSM and the relations between generator polynomials and FSM-state/input.

The resulting trellis is well-known and time-invariant as in each time step the same relation between input value, FSM state, and generator polynomials holds.

#### B. Matched Decoding

In the following, we recall the matched decoding approach briefly. As we derived in [3], the matched decoding approach combines the channel encoder with the ISI-channel in such a way, that fewer states are sufficient to describe the super-trellis. There, the rate- $K/n$  convolutional code was matched to a  $2^n$ -ary ASK-transmission scheme. Instead of creating the super-trellis based on the  $M$ -ary channel, we represented the super-trellis based on  $\log_2 M = n$  parallel binary ISI-channels. With  $C = -\sum_{k=0}^L h[k](M-1)$  and the Gauss representation of the modulo operation the transmission can be represented as depicted in Fig. 3. There, the memory of the ISI-channel is binary only and a natural labeling is performed. This approach enables a first state reduction of the super-trellis without loss in minimum Euclidean distance.

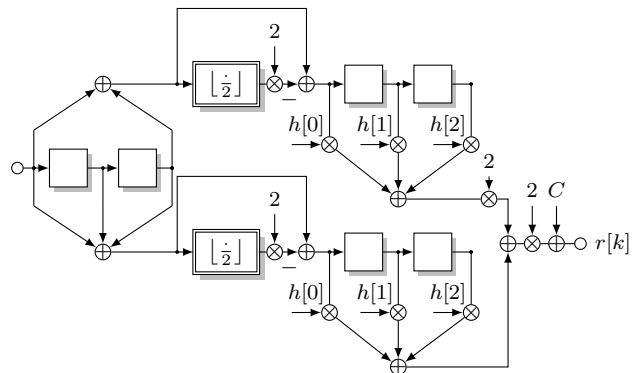


Fig. 3: Replacement of the mod 2 addition with the non-linear representation using floor function. ( $M = 4$ , *i.e.*,  $n = 2$ , *non-punctured* code).

Figure 4 illustrates the state transitions of the transmitter FSM when *non-punctured* convolutional encoding and ISI-channel are considered jointly.

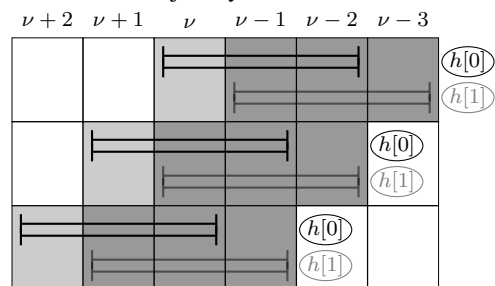


Fig. 4: State transitions of the FSM for matched decoding.

### IV. MATCHED DECODING FOR PUNCTURED CODES

We now describe the encoding process and state transitions when *punctured codes* are used. We will discuss the FSM for punctured convolutional codes as well as the modifications necessary for the VA to run in the resulting trellis.

### A. Description of the Finite State Machine

When punctured convolutional codes are used, the strict relation between an uncoded information bit,  $n$  encoded bits and the mapped symbol is no longer valid. As can be seen from Fig. 5 (top), the third and seventh encoded symbol, for example, are punctured and do not contribute to the mapping process. Additionally, there is no strict relation between MSB, LSB and the output of the generator polynomials, anymore. The transitions of the FSM, depicted in Fig. 5 (bottom), show three differences when compared to *non-punctured* FSM transitions, cf. Fig. 2 (bottom). These are described subsequently.

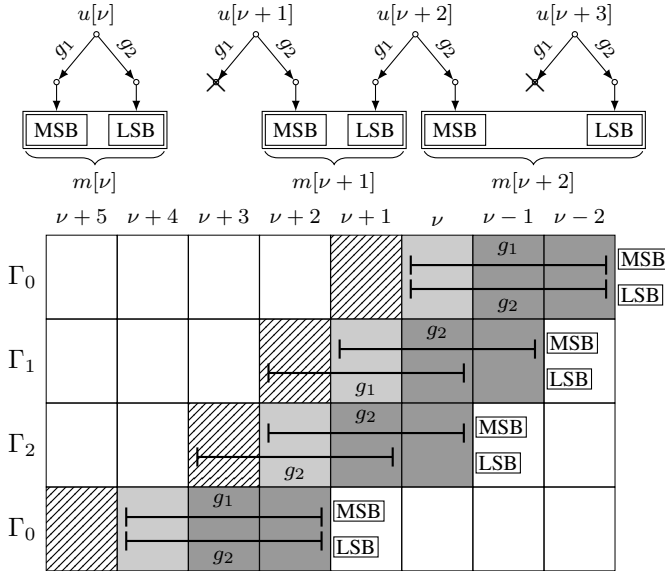


Fig. 5: Top: Encoding process for a rate-2/3 punctured convolutional code and natural labeling. Overall transmission rate  $R = 4/3$ . Bottom: State transitions of the transmitter FSM and the relations between generator polynomials and FSM-state/input.

1) *Generator Offsets  $\Gamma_i$* : It becomes clear that the strict relation between the MSB, LSB and the generator polynomial  $g_1$  and  $g_2$ , respectively, no longer hold. The second symbol, *i.e.*,  $m[\nu+1]$ , for example, contains information about  $u[\nu+1]$  and  $u[\nu+2]$ . In addition, the MSB is now generated by  $g_2$  instead of  $g_1$  as was the case in the *non-punctured* approach. Accordingly, the LSB, which was generated by  $g_2$  in the *non-punctured* case, is now generated by  $g_1$ . It is also clear that the third symbol is generated by  $u[\nu+2]$  and  $u[\nu+3]$  using the generator polynomial  $g_2$  twice.

To handle these relations we introduce a set of so called generator offsets  $\Gamma_i$  which describe, depending on the puncturing scheme, the relations between generator polynomials, input value, FSM state, and mapping to MSB or LSB, respectively. For example,  $\Gamma_1$  indicates that the MSB output symbol is generated with the input value (light gray), the FSM state, and the generator polynomial  $g_2$ . On the other hand, to calculate the LSB we have to use the extension (hatched block,  $\text{hatched}$ ) as input value so that  $g_1$  is one step ahead of the LSB. Therefore, the input value for the MSB is now part of the FSM state for the LSB. Note that, in the case of  $M = 4$ ,  $\Gamma_0$  is used

whenever no effect occurs for puncturing, *i.e.*, an even number of puncturings occurred up to time instant  $\nu$ , and the generator polynomials are synchronized with LSB and MSB.  $\Gamma_1$  is used, whenever an odd number of puncturings has happened and  $\Gamma_2$  is used when an additional puncturing synchronize the generator polynomials with MSB and LSB again. The number of generator offsets needed to describe all steps depends on the size of the modulation alphabet whereas the generator offsets depend also on the puncturing scheme.

2) *State Extension*: The FSM transitions in Fig. 5 (bottom) show that the symbol  $m[\nu+1]$  contains information on the uncoded information bits  $u[\nu+1]$ , for which the MSB output was punctured, and the consecutive information bit  $u[\nu+2]$ . We see that, when generating the output, the calculation of the LSB is one step ahead to the MSB and considers one extra information bit. This results in a trellis that has to be expanded (*i.e.*, splitted) by a factor of two. This can be easily seen from the figure as the generator polynomials in the second step (generator offsets  $\Gamma_1$ ) now cover four blocks instead of just three. However, for a 4-ary transmission, when puncturing happens a second time, MSB and LSB are resynchronized with the generator polynomials and a so called merge happens in the trellis diagram.

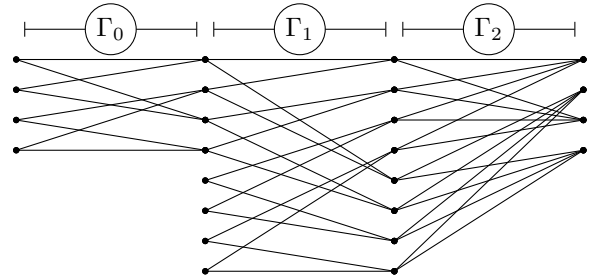


Fig. 6: Super-trellis representation for a punctured rate-2/3 convolutional code. In the first to VA steps, two transitions arrive at each state, *i.e.*, one bit can be estimate, whereas the third step allows an estimation for two bits.

Therefore, a trellis based decoding algorithm, such as the VA, has to be performed on a time-variant trellis diagram. As an example, Fig. 6 shows the resulting trellis diagram for a punctured convolutional code with a constraint length  $\nu = 2$ .

3) *Time Asynchronicity*: The punctured code has a rate of  $R_p = 2/3$ . As we can not insert Log-Likelihood Ratios (LLR) with  $\mathcal{L} = 0$  after equalization and before decoding, because of the joint trellises of equalization and decoding, the VA has to estimate four bits from just three received symbols to achieve the code rate. As one can see from the trellis in Fig. 6 the first two steps  $\Gamma_0$  have two transitions arriving at each state resulting in an estimation of a single bit per state. However, the last step  $\Gamma_2$  has four transitions into each state so that the decision for a survivor gives an estimate on two bits. The path register of the VA has to consider the fact that now four bits have been estimated within three received symbols. The last step can be described as a state merging, whereas the split is performed in the first step, *e.g.* by copying the state metrics of the first four states into the last four states.

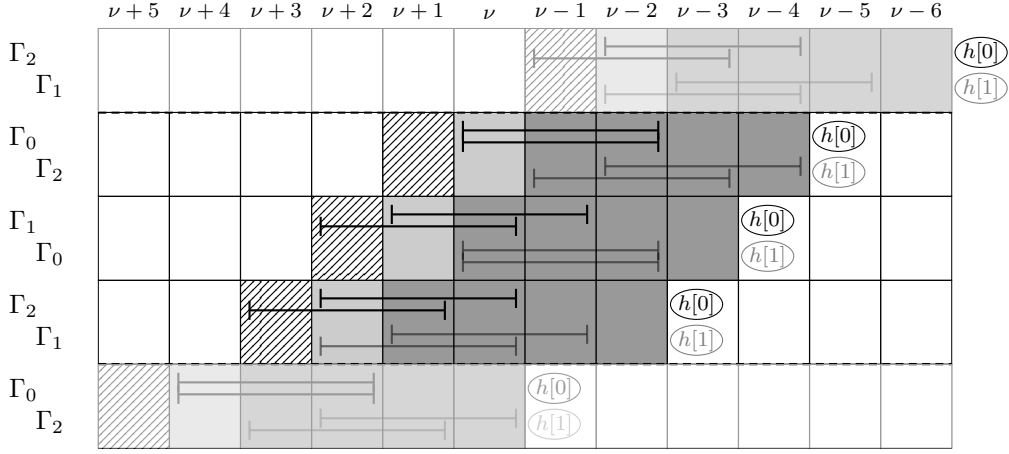


Fig. 7: State transitions of the transmitter FSM with  $R = 4/3$  and the relations between generator polynomials, FSM-state/input and channel state for a memory-1 ISI-channel.

### B. Viterbi Modifications for Punctured Codes

As mentioned above the VA has to estimate four bits within three symbols from the trellis transitions. To see the modifications of the VA we need to consider the state extension.

Using Fig. 5 (bottom), we define in each step  $\Gamma_0, \dots, \Gamma_2$  the input value to be the first value which is used by either  $g_1$  or  $g_2$ . As a result, in step  $\Gamma_0$  the values at time instants  $k = \{\nu; \nu + 4\}$  can be defined as input values. When in step  $\Gamma_1$  or  $\Gamma_2$ , the input value is at time instant  $k = \{\nu + 2; \nu + 3\}$  (e.g., the hatched values,  $\text{\textcircled{X}}$ ). Unfortunately we can not estimate the input value  $u[\nu + 2]$  in  $\Gamma_1$  because parts of the information has not been received, yet, (i.e., missing information is located in the MSB in  $\Gamma_2$ ). However, as all information on  $u[\nu + 1]$  (for which the output of  $g_1$  was punctured) has been received we can estimate it. To do so we have to evaluate the most significant bit of the survivor state which is selected by the VA. In  $\Gamma_2$ , as already mentioned, selecting the survivor path allows a decision for two information bits (the most significant bit of the survivor *and* the input value) because four transitions end in each state, here. For implementations, keep in mind that the VA is thus running asynchronously to the desired information sequence at the output to achieve the overall rate  $R = 4/3$ .

### C. Matched Decoding

The above description now enables the extension for super-trellis decoding of punctured convolutional coded transmission over ISI-channels. To extend matched decoding for punctured codes, one must ensure that the right generator offsets  $\Gamma_i$  are involved at the right time. Once the encoding and mapping is executed (here natural labeling and 4-ASK modulation are considered), the symbols traverse through the ISI-channel independent from the encoding and puncturing process. For an ISI-channel with two taps (channel memory  $L = 1$ ), for example, two output symbols of the mapper are involved at each time instant. Thus, two out of the existing three generator offsets  $\Gamma_i$  and  $\Gamma_{(i-1) \bmod 3}$  have to be considered.

This can be seen from Fig. 7. For a memory-1 channel, in the third step (generator offset  $\Gamma_2$ ),  $m[\nu+2]$  is received and the ISI-channel memory contains  $m[\nu+1]$  which was generated

in the previous time instant using generator offset  $\Gamma_1$ . The resulting overall generator offsets are depicted in Fig. 7. This scheme can easily be extended to arbitrary lengths of the ISI-channel.

## V. NUMERICAL RESULTS

The effectiveness of the approach of punctured MD is now verified by means of numerical simulations. We restrict ourselves to rate- $1/2$  encoding schemes and a 4-ary modulation alphabet. As convolutional encoder we apply the generator polynomials  $[5_{\text{oct}}; 7_{\text{oct}}]$  which, in combination with Gray labeling, results in a trellis coded modulation scheme (TCM) for  $M$ -ary ASK. The puncturing scheme is defined as  $P_1 = \{1; 0\}$  and  $P_2 = \{1; 1\}$  as shown in Figure 1 and 5. Thus, the overall transmission rate is  $R = 4/3$ . Please note, that this combination of encoder, puncturing scheme, and mapper may not be the optimum choice. However, it allows a comprehensible description of our approach.

For simplicity an exemplary minimum phase ISI-channel is generated by

$$h[k] = \frac{1}{\alpha} \cdot \frac{L - k + 1}{L + 1}; \quad 0 \leq k \leq L \quad (1)$$

$$\alpha^2 = \sum_{k=0}^L \left( \frac{L - k + 1}{L + 1} \right)^2 \quad (2)$$

and normalized to unit energy. Please note that due to the normalization the equivalent energy per bit  $E_b$  is identical at transmitter output and receiver input. The applied ISI-channel is described by (1) using  $L \in \{2; 3; 4\}$  with  $Z_{\text{cha}} = \{16; 64; 256\}$  states, respectively.

The simulation results in Fig. 8 shown the bit error rate (BER) over an ISI-AWGN-channel with ratio of energy per information bit and one-sided power spectral density  $\frac{E_b}{N_0}$ .

Our MD approach of the VA operating on the time-variant equivalent non-linear trellis description is compared to separate equalization and decoding employing DFSE/BCJR [6] for equalization and full-state VA for decoding. Please note that by dispensing the interleaver between channel encoding and modulation for the separated approaches, block errors that

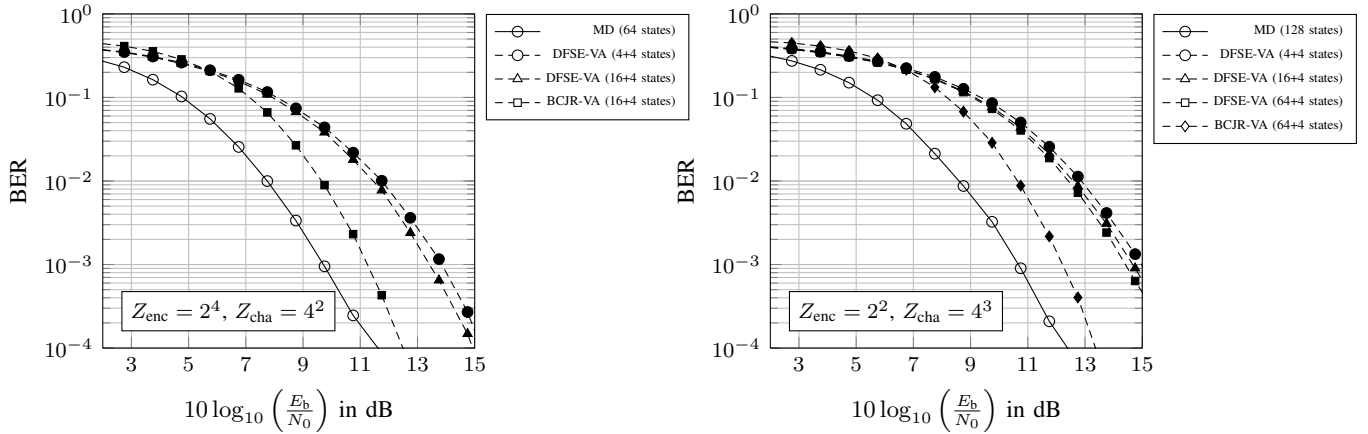


Fig. 8: Bit error performance for convolutionally encoded 4-ASK transmission (gray labeling) with overall rate  $R = 4/3$  over the ISI-AWGN-channel. Generator polynomials  $[5_{\text{oct}}; 7_{\text{oct}}]$  ( $Z_{\text{cha}} = 4$ ). Left: Memory-2 ISI-channel ( $L = 2$ , *i.e.*,  $Z_{\text{cha}} = 16$ ). Right: Memory-3 ISI-channel ( $L = 3$ , *i.e.*,  $Z_{\text{cha}} = 64$ ).

are caused by the equalization process reduce the ability to decode due to correlated errors. Obviously, the soft-decision separated approach results in improved bit error rates when compared to to hard-decision separated approach. However, the separated equalization and decoding approach is significantly outperformed by MD as decoding is carried out in the super-trellis. Note that the results are well-known for super-trellis decoding but are achieved with fewer states due to the equivalent non-linear trellis description.

We also conducted simulations for larger trellises as shown in Fig. 9. There, the convolutional code can be described with a four-state FSM and the ISI-channel has five taps resulting in 256 states, for a 4-ary ASK-transmission. In the case of a *non-punctured* code the straight-forward super-trellis has 1024 states. The matched decoding approach reduces the super-trellis to only 64 states using a non-linear trellis description [3]. However, for a punctured convolutional code, the time-variant super-trellis would have 1024 states, and 2048 states when splitted. The matched decoding approach allows a state reduction to 256 and 512 states, respectively. Apparently, already for moderate encoder size and short ISI-channels, super-trellis decoding becomes intractable, when the code is punctured due to the state expansion.

Therefore, we also implemented an algorithm to perform the VA on a reduced set of states. Due to lack of space we can not describe the modification to the reduced-state sequence estimation (RSSE) in full detail, here. The state partitioning needed for RSSE uses the minimum-phase characteristic of the impulse response of the ISI-channel and can be related to decision feed-back sequence estimation, a partial solution of RSSE. A detailed description on the application of RSSE of *non-punctured* convolutional codes can be found in [3].

The simulation results shown in Fig. 9 indicate, that our MD-RSSE approach for punctured convolutional codes enables efficient super-trellis decoding and also allows a trade-off between complexity and performance, *i.e.*, noise-robustness can be achieved. Obviously, the proposed decoding scheme significantly supersedes the separated equalization and decoding approaches already for only 16 states.

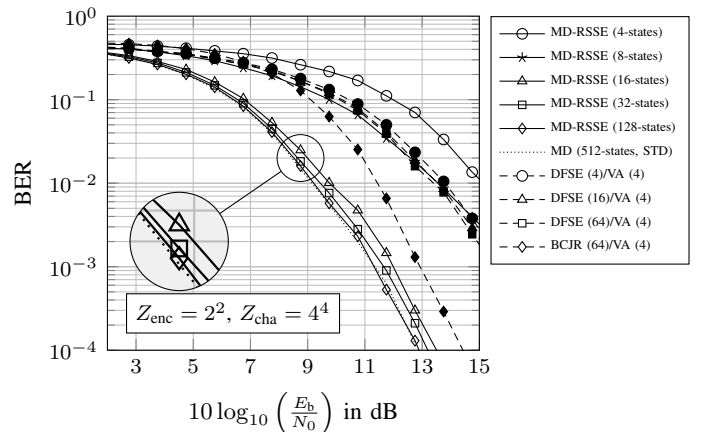


Fig. 9: Bit error performance for convolutionally encoded 4-ASK transmission (gray labeling) with overall rate  $R = 4/3$  over memory-4 the ISI-AWGN-channel ( $Z_{\text{cha}} = 256$ ) with Generator polynomials  $[5_{\text{oct}}; 7_{\text{oct}}]$  ( $L = 4$ , *i.e.*,  $Z_{\text{cha}} = 256$ ).

## VI. CONCLUSION

In this paper we have shown that it is possible to perform trellis decoding of punctured convolutional encoded transmissions. We extended the well-known decoding approach for the use over ISI-channels and described the differences of matched decoding between non-punctured and punctured codes. By using RSSE with DFSE-like partitioning we obtain an efficient method for a trade-off between complexity and performance.

## REFERENCES

- [1] T. Hehn and J. Huber, "LDPC Codes and Convolutional Codes with Equal Structural Delay: A Comparison," *IEEE Transactions on Communications*, vol. 57, no. 6, pp. 1683–1692, Jun. 2009.
- [2] E. Zehavi, "8-PSK Trellis Codes for a Rayleigh Channel," *Communications, IEEE Transactions on*, vol. 40, no. 5, pp. 873–884, May 1992.
- [3] F. Schuh, A. Schenk, and J. Huber, "Reduced Complexity Super-Trellis Decoding for Convolutionally Encoded Transmission Over ISI-Channels," *ArXiv e-prints*, Jul. 2012.
- [4] J. Huber, *Trelliscodierung: Grundlagen und Anwendungen in der digitalen Übertragungstechnik*. Springer, 1992.
- [5] A. Viterbi, "Error Bounds for Convolutional Codes and an Asymptotically Optimum Decoding Algorithm," *Information Theory, IEEE Transactions on*, vol. 13, no. 2, pp. 260–269, Apr. 1967.
- [6] L. Bahl, J. Cocke, F. Jelinek, and J. Raviv, "Optimal Decoding of Linear Codes for Minimizing Symbol Error Rate (Corresp.)," *Information Theory, IEEE Transactions on*, vol. 20, no. 2, pp. 284–287, Mar. 1974.